Crimson Publishers
Wings to the Research

Research Article

Estimation of Ductile-Brittle Transition Temperature Using Small Punch Test in Aged Gas Pipes

Milad Z Aghdam[1]*, Nasser Soltani[2], Mostafa Khodaie[1], Mohammad J Sohrabi[3] and Hadi Nobakhti[1]

[1]Research Assistant, Intelligence Based of Experimental Mechanics (IBEM), School of Mechanical Engineering, College of Engineering, University of Tehran, Iran

[2]Professor, Faculty of Mechanical Engineering, College of Engineering, University of Tehran, Iran

[3]PhD Candidate, School of Metallurgy and Materials Engineering, College of Engineering, University of Tehran, Iran

ISSN: 2640-9690

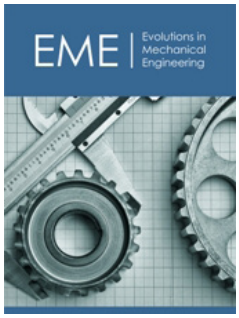

***Corresponding author:** Milad Z Aghdam, Research Assistant, Intelligence Based of Experimental Mechanics (IBEM), School of Mechanical Engineering, College of Engineering, University of Tehran, Iran

Submission: January 27, 2025
Published: February 24, 2025

Volume 5 - Issue 5

How to cite this article: Milad Z Aghdam*, Nasser Soltani, Mostafa Khodaie, Mohammad J Sohrabi and Hadi Nobakhti. Estimation of Ductile-Brittle Transition Temperature Using Small Punch Test in Aged Gas Pipes. Evolutions Mech Eng. 5(5). EME.000625. 2025.
DOI: 10.31031/EME.2025.05.000625

Abstract

Ductile to Brittle Transition Temperature (DBTT) is an important parameter that can be estimated using the Small Punch Test (SPT) utilized in material assessment in industrial structures without significant destruction. This study applies the SPT method to determine DBTT in austenitic/martensitic stainless steel from a gas pipe system that worked for around 20 years at low temperatures and is prone to material degradation due to hydrogen effects and aging. SPTs were conducted at temperatures from -196 to 50 degrees on specimens extracted from the most damage-prone areas on the inner side of the gas pipe. Fracture energies were measured by calculating the area under force-displacement curves obtained SPT. The small punch transition temperature was determined at the middle zone of the upper and lower shelves, being -40 degrees. It was clear from the fracture area and surface using SEM investigations that the material ductile fracture alters to brittle by temperature decrease

Keywords: Fracture mechanics; Ductile to brittle transition temperature (DBTT); Small punch test; Stainless steel; Gas pipe

Introduction

Temperature plays an undisputable role in material failure, particularly in fracture mode. From the Second World War and lots of failures in cargo ships due to cold environments, it was figured out that the fracture energy in materials drops by decrease in temperature. This drop occurs at a certain temperature called Ductile to Brittle Transition Temperature (DBTT). This phenomenon is very important in ferritic steels [1], and finding the DBTT is considerably important to designing products and predicting future failures [2,3].

DBTT is important in all industrial structures to estimate the fracture properties and failure. This topic has attracted engineers to predict and postpone pipe failures, particularly gas pipes that experience low temperatures and are prone to catastrophic bursts. Hence, various efforts were made to determine the DBTT in pipes. With this regard, for example, Samal et al. [4] found the master curve in ferritic grade low-alloy steels used in pressure vessels. The steel was highly degraded due to irradiation embrittlement and material aging. The DBTT was also focused on pipeline weld areas [5]. In this study, the Charpy method estimated the DBTT in the affected zone area in the girth welded joints. In another study, Shang et al. [6] proposed a quantitative expression for DBTT in pipeline systems. They collected data and employed machine learning methods to derive the relation for the DBTT. The SPT is test method that

was introduced in the 1980s [7] is popular due to the small size of the specimen. This test is employed for material characterization from various points of view, namely determination of mechanical properties such as yield stress [8-10], ultimate stress [11-13], fracture properties [14,15], fatigue [16,17] and creep [18-20].

The SPT is also used for the evaluation of DBTT which is an essential parameter in the field of fracture mechanics. DBTT measurement is conventionally done by Charpy V-Notch impact test (CVN), while it needs a considerable amount of material and a considerable effort for specimen preparation and testing. Hence, the SPT is a favourable alternative for the CVN. SPT is able to determine the DBTT [21], but the DBTT (T_{sp}) obtained from SPT is considerably lower than obtained from the CVN (T_{CVN}) [22,23]. However, there have been numerous successful studies to draw a relationship between T_{sp} and T_{CVN}, leading to a linear relation between these two temperatures [24-28]. In this linear relation, the T_{sp} is simply determined by multiplying a factor in T_{CVN}. This factor was reported around 0.4 in the literature [29,25,30]. Additionally, other quadratic nonlinear relationships have also been reported [31,32]. The current study aims to determine the DBTT in the stainless-steel gas pipe system. The pipe experienced degradation in mechanical and decrease of fracture properties due to damages caused by erosion, hydrogen affect, and other factors during the long service time. To this end, first, a few SPT specimens were removed from the inner surface of the gas pipe and were then prepared and tested at various temperatures from -196 to +50 degrees. These temperatures are achieved by adding liquid nitrogen to the SPT setup located in a chamber. T_{spwas} determined where the fracture energy is in the middle of the upper and the lower shelf.

Material and Experiment

Gas pipes are prone to material degradation due to contact with gas, environmental effects, mechanical and temperature fatigue effects, aging problems and others. With this regard, hydrogen-induced degradation is of the essence in all pipeline system components due to the contact of material with natural gas [33]. Hydrogen may be taken up by carbon steels, leading to various degradations, and material embrittlement is their most important mode. Hydrogen causes considerable loss in steel ductility, particularly in the presence of stresses [34]. Moreover, hydrogen can decrease fracture toughness and speed up crack growth [35]. Hence, studying material fracture toughness after degradation is significant in gas pipe systems. This study aims to determine the DBTT of the pipe material, which is stainless steel, used for natural gas pipeline systems. The pipe has been in service for a long time, around 20 years, and has been under hydrogen and loading effects during this time. Thus, the material properties have been changed due to degradation. Thus, the material DBTT should be studied because pipes experience various temperatures due to changes in natural gas pressure. To this end, SPT specimens are extracted from the inner surface of a gas pipe (Figure 1). By the SPT method, the pipe does not experience severe destruction and the area that the specimen was extracted from can be repaired with a patch. The chemical composition of materials is shown in Table 1. XRD is also used to determine material phase fractions (Figure 2). According to this result, around 45 percent of the material is a martensitic phase. The SPT specimen is a disc with 10mm or 8mm diameter and 0.5mm thickness. Figure 3 illustrates an SPT setup in which the specimen is clamped by two dies. The force is applied by a puncher to a 2.5mm ball that is penetrated to the specimen. The result is a force-displacement curve whereby mechanical properties are determined through correlation with standard tests. Figure 4 shows the setup with a chamber and temperature controller to hold the temperature steady. There are two steps for T_{sp} determination. The first is to calculate the fracture energy from force-displacement curves at different temperatures.

Figure 1: The inner side of the gas pipe.

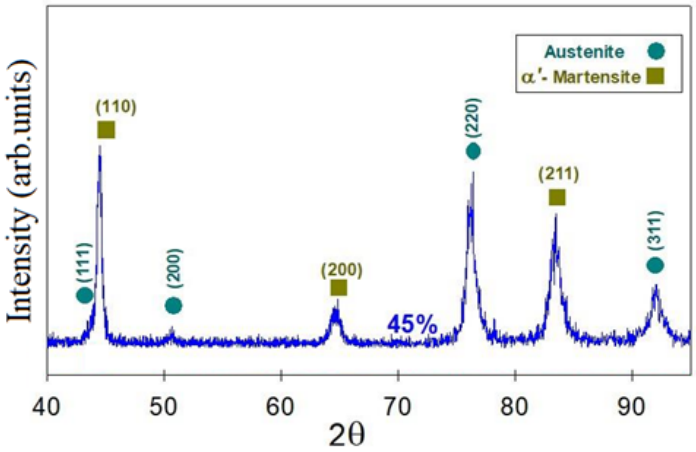

Figure 2: XRD result for phase fraction determination.

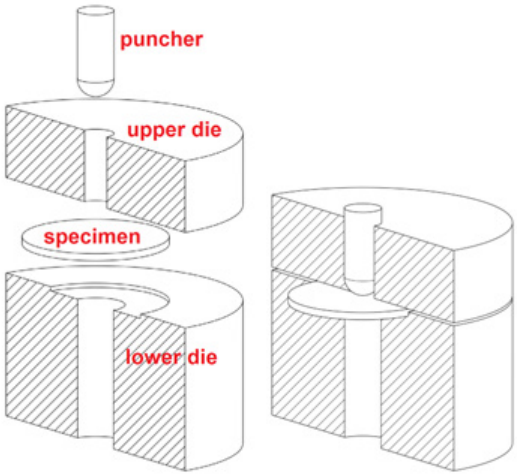

Figure 3: SPT setup and specimen.

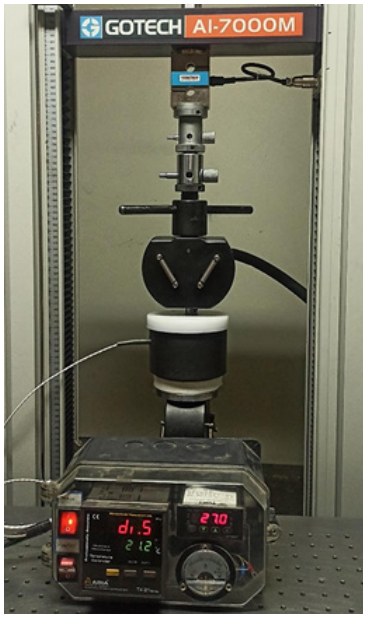

Figure 4: SPT setup with cooling chamber.

Table 1: Chemical composition of material.

Fe	C	Si	Mn	P	S	Cr
Base	0.07	0.49	1.21	0.025	0.006	18.15
Mo	**Ni**	**Co**	**Cu**	**Nb**	**V**	**W**
0.03	8.04	0.21	0.12	0.014	0.11	0.02

This energy is calculated by the following equation:

$$E_{sp} = \int_0^{uf} F(u)du \quad (2\text{-}1)$$

where the F(u) is the force applied to the specimen at displacement represented by 'u'. u_f is the displacement where the force reaches to the maximum force [29,36], or passes it and reaches 80% of the maximum force [37]. E_{sp} drops at DBTT and two shelves of energy are seen. The upper shelf before DBTT and the lower after that. The DBTT is the average of temperatures related to these two shelves. To reach a better comparison between the two shelves the fracture energy is normalized by the following equation:

$$E_n = \frac{E_{sp}}{T} \quad (2\text{-}2)$$

Where T is the test temperature and E_n is normalized energy. This equation divides the Fracture energy to the temperature. This process can help the scientist to achieve a better contrast between the upper shelf and the lower one, simplifying the estimation of the DBTT [38].

Results and Discussion

SPTs were performed at various temperatures from -196 to 50°C by a setup working based on liquid nitrogen. To achieve more accurate results, three specimens were tested for each temperature. Force-displacement curves are shown in Figure 5. Obviously, the maximum force, failure displacement and fracture energy decrease with temperature reduction. Figure 6 shows the failure displacements at each temperature. Clearly, at 25 °C temperature and 50 °C the fracture displacements are above 2mm. In -10 °C the number comes under 2mm, followed by the second reduction to 1.5mm for -40 °C. The reduction gradually continues to more than 1mm at -130 °C, -160 °C and -196 °C. Fracture energy (E_{sp})and normalized fracture energy (E_n) at various temperatures are shown in Figure 7 & 8. Taking the average of upper and lower shelves as the transition point, which is illustrated by two horizontal lines, it occurs at a temperature near -40 °C. Using this temperature and what is reported in the literature the T_{CVN} can be estimated. The fracture energy is approximately 0.8mJ/N. Figure 9 shows the fracture area in SPT specimens with colours representing the temperatures. Obviously, in 25 °C and 50 °C there is a 2mm height hill and fracture occurs at the hillside [39]. The fracture surface at 50 °C is shown in Figure 10. Spalling is clear at the fracture surface, meaning that the failure is ductile. Additionally, Figure 11 shows the fracture surface at -196 °C. In this case, the fracture is obviously brittle. It is also obvious from Figure 8 that the fracture occurs at small deflection due to the brittleness.

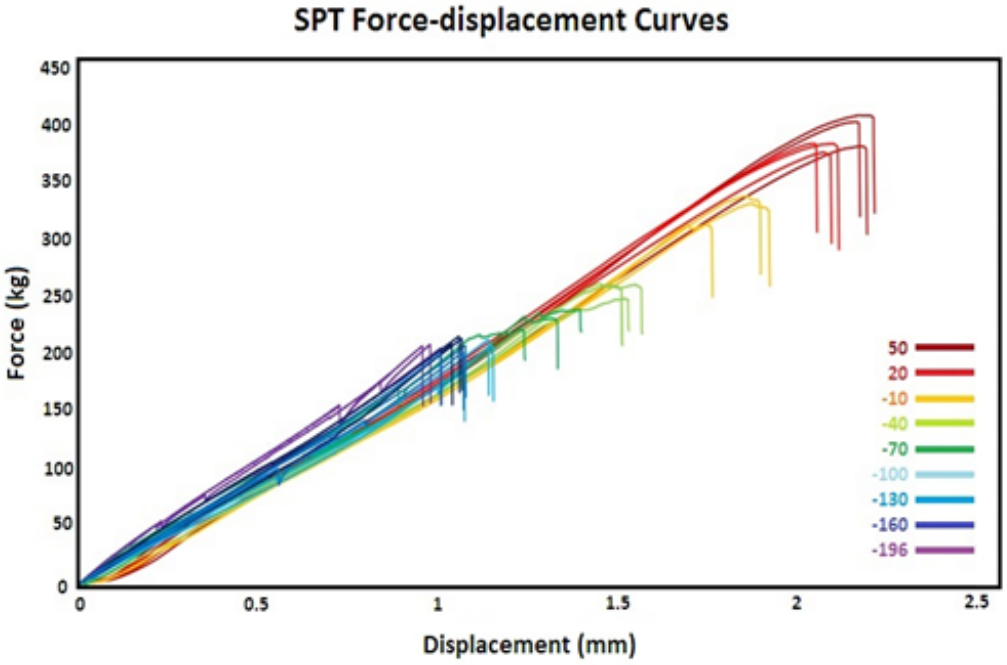

Figure 5: SPT force-displacement curves in various temperatures.

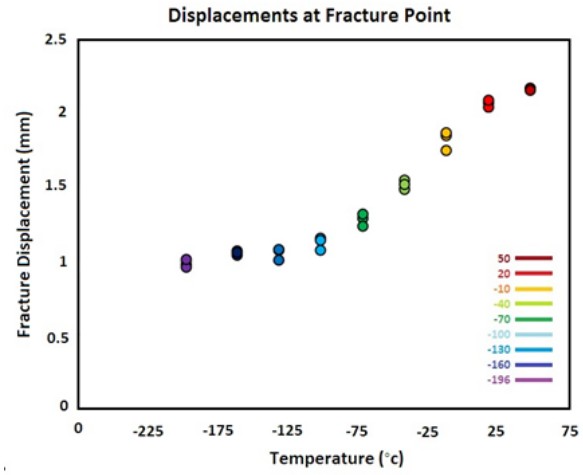

Figure 6: Failure displacements at various temperatures.

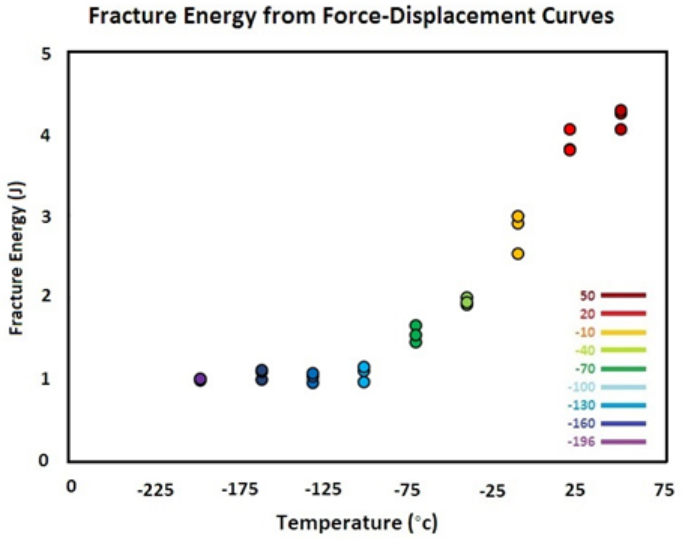

Figure 7: Fracture energy measured at various temperatures from SPT curves.

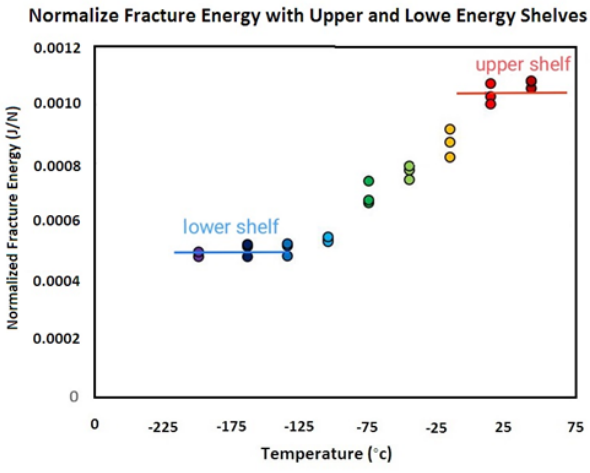

Figure 8: Normalized fracture energy.

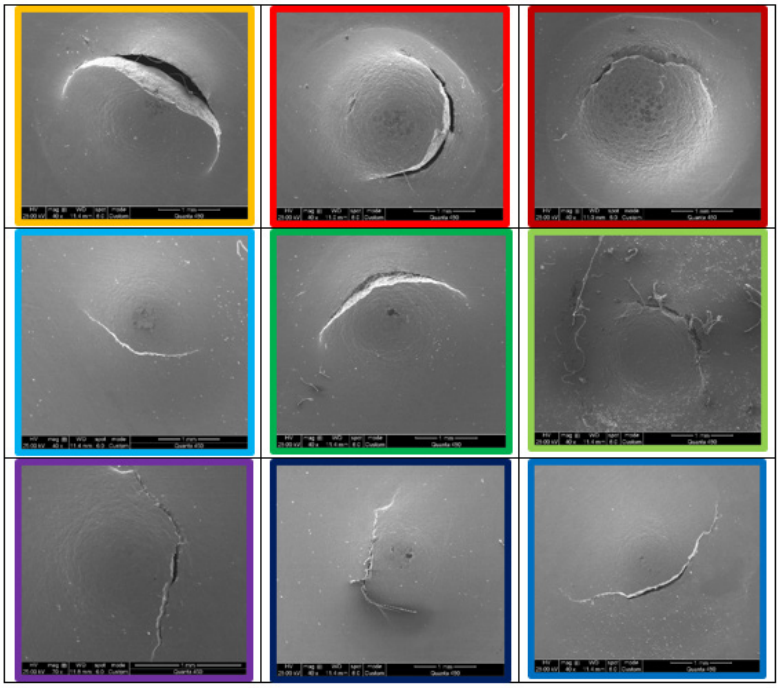

Figure 9: SEM images from fracture areas in various temperatures.

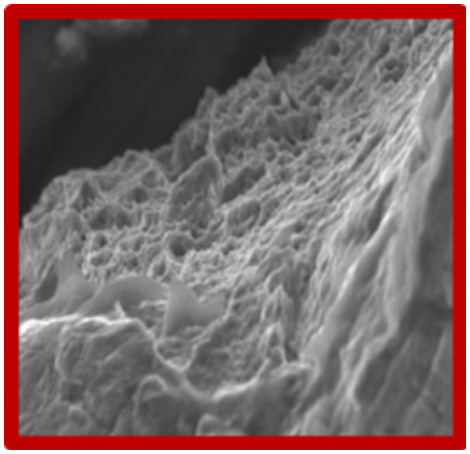

Figure 10: Fracture surface at 50 °C.

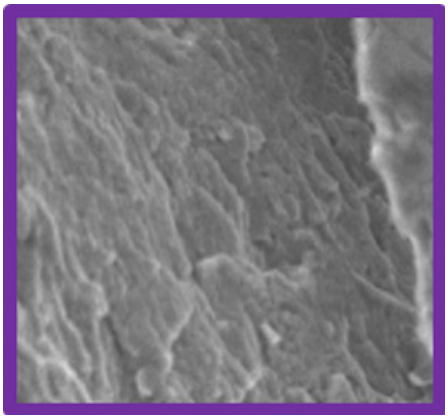

Figure 11: Fracture surface at -196 °C.

Conclusion

The study focused on a DBTT measurement in stainless steel from a damaged gas pipe. To this end:

a. SPT Specimens were removed from the pipe inner surface.

b. Material composition was first determined by material chemical analysis.

c. The austenitic/martensitic phase fraction was determined through the XRD technique

d. After specimen preparation, the SPT tests were performed at various points from -196 °C to 50 °C, and the force-displacement curves were plotted.

e. Fracture displacements and fracture energies at various temperatures were calculated by the area under force-displacement curves.

f. Using normalized fracture energies, the DBTT temperature was calculated.

g. Finally, the fracture surface was investigated using SEM images, resulting in a clear transition from ductile to brittle.

References

1. RK Barik, A Ghosh, D Chakrabarti (2023) Fundamental insights on ductile to brittle transition phenomenon in ferritic steel. Materialia 27: 101667.
2. A Maksimović, L Milović, B Zečević, V Aleksić, D Bekrić (2024) Determination of the ductile-to-brittle transition temperature of NIOMOL 490K steel welded joints. Theoretical and Applied Fracture Mechanics 42: 1361-1368.
3. KC Le, H Jeong, TM Tran (2023) Theory of transition from brittle to ductile fracture. Physical Review E 107(5):

4. MK Samal, JK Chakravartty, M Seidenfuss, E Roos (2011) Evaluation of fracture toughness and its scatter in the DBTT region of different types of pressure vessel steels. Engineering Failure Analysis 18(1): 172-185.
5. Jang Bog Ju, Woo-Sik Kim, Jae-il Jang (2012) Variations in DBTT and CTOD within weld heat-affected zone of API X65 pipeline steel. Materials Science and Engineering: A 546: 258-262.
6. Chunlei Shang, Zhu D, Hui Wu, H, Bai P, Hou F, et al. (2024) A quantitative relation for the ductile-brittle transition temperature in pipeline steel. Scripta Materialia 244: 116023.
7. MP Manahan, AS Argon, OK Harling (1981) The development of a miniaturized disk bend test for the determination of post irradiation mechanical properties. Journal of Nuclear Material 104: 1545-1550.
8. J Kameda, X Mao (1992) Small-punch and TEM-disc testing techniques and their application to characterization of radiation damage. Journal of Material Science 27: 983-989.
9. P Hähner, C Soyarslan, BG Çakan, S Bargmann (2019) Determining tensile yield stresses from small punch tests: A numerical-based scheme. Materials & Design 182: 107974.
10. CA León-Patiño, RJ González-Esquivel, DU Hernández-Huerta, EA Aguilar-Reyes (2023) Microstructural characterization and tensile strength of TiC/Ni-20Cr composite through the small punch test technique. Journal of Materials Engineering and Performance 8: 46-51.
11. Altstadt E, Houska M, Simonovski I, Bruchhausen M, Holmstr S (136) On the estimation of ultimate tensile stress from small punch testing. International Journal of Mechanical Sciences 136: 85-93.
12. J Calaf Chica, P Bravo Díez, M Preciado Calzada (2018) A new prediction method for the ultimate tensile strength of steel alloys with small punch test. Materials 11(9): 1-16.
13. Y Cao, C Ren, Y Zu, Y Zhen (2023) Quantitative characterization of strength properties of girth welded joints based on small punch test. Journal of Materials Engineering and Performance 33: 12561-12572.
14. R Lacalle, D Andres, JA Alvarez, F Guti (2017) Transition region of nuclear vessel steels: Master curve approach using small punch notched specimens. Key Engineering Materials 734: 77-86.
15. MZ Aghdam, N Soltani, R Rahman, H Nobahkti (2024) Fracture resistance measurement in small punch test supported by optical monitoring device. Journal of Mechanical Science and Technology 38(11): 6039-6045.
16. RJ Lancaster, SP Jeffs, HW Illsley, C Argyrakis, RC Hurst, et al. (2019) Development of a novel methodology to study fatigue properties using the small punch test. Materials Science and Engineering: A 748: 21-29.
17. DTS Lewis, RJ Lancaster, SP Jeffs, HW Illsley, SJ Davies, et al. (2019) Characterising the fatigue performance of additive materials using the small punch test. Material Science and Engineering: A 754: 719-727.
18. A Moradi, N Soltani, H Nobakhti (2017) Experimental study of remaining creep life of SA-304L stainless steel using small punch creep test. Materials at High Temperatures 35(5): 410-417.
19. H Nobakhti, N Soltani (2016) Evaluating small punch test as accelerated creep test using Larson-miller parameter. Experimental Technique 40: 645-650.
20. S Kim, U Ro, YH Kim, T Lee, MK Kim (2022) Evaluation of creep properties using small punch creep test for modified 9Cr-1Mo steel. Journal of Mechanical Science and Technology 36: 4549-4561.
21. J Kameda, O Buck (1986) Evaluation of the ductile-to-brittle transition temperature shift due to temper embrittlement and neutron irradiation by means of a small-punch test. Material Science and Engineering 83(1): 29-38.
22. K Turba, B Gulcimen, YZ Li, D Blagoeva, P Hähner, et al. (2011) Introduction of a new notched specimen geometry to determine fracture properties by small punch testing. Engineering Fracture Mechanics 78(16): 2826-2833.
23. MA Contreras, C Rodríguez, F Belzunce, C Betegón (2008) Use of the small punch test to determine the ductile-to-brittle transition temperature of structural steels. Fatigue and Fracture of Engineering Materials and Structures 31(9): 727-737.
24. M Saucedo-Muñoz, T Matsushita, T Hashida, T Shoji, H Takahashi (2000) Development of a multiple linear regression model to estimate the ductile-brittle transition temperature of ferritic low-alloy steels based on the relationship between small punch and V-Notch tests. Journal of Testing Evaluation 28(5): 352-358.
25. X Jia, Y Dai (2003) Small punch tests on martensitic/ferritic steels F82H, T91 and Optimax-A irradiated in SINQ Target-3. Journal of Nuclear Material 323(2-3): 360-367.
26. M Saucedo-Muñoz, T Hashida, T Shoji, V Lopez-Hirata (2012) Correlation between small punch and CVN impact tests for evaluation of cryogenic fracture characteristics of isothermally-aged nitrogen-containing austenitic stainless steels. Materials Research's 15(2): 218-223.
27. B Gülçimen, A Durmus, S Ülkü, RC Hurstc, K Turba, et al. (2013) Mechanical characterisation of a P91 weldment by means of small punch fracture testing. International Journal of Pressure Vessels and Piping 105-106: 28-35.
28. K Turba, R Hurst, P Hähner (2013) Evaluation of the ductile-brittle transition temperature in the NESC-I material using small punch testing. International Journal of Pressure Vessels and Piping 111-112: 155-161.
29. T Misawa, T Adachi, M Saito, Y Hamaguchi (1987) Small punch tests for evaluating ductile-brittle transition behaviour of irradiated ferritic steels. Journal of Nuclear Materials 150(2): 194-202.
30. M Kim, YJ Oh, BS Lee (2005) Evaluation of ductile-brittle transition temperature before and after neutron irradiation for RPV steels using small punch tests. Nuclear Engineering and Design 235(17-19): 1799-1805.
31. JH Bulloch (1998) Toughness losses in low alloy steels at high temperatures: An appraisal of certain factors concerning the small punch test. International Journal of Pressure Vessels and Piping 75(11): 791-804.
32. JH Bulloch (2002) A review of the ESB small punch test data on various plant components with special emphasis on fractographic details. Engineering Failure Analysis 9(5): 511-534.
33. H Nykyforchyn, O Zvirko, I Dzioba, H Krechkovska, M Hredil, et al. (2021) Assessment of operational degradation of pipeline steels. Materials 14(12): 3247.
34. A Laureys, T Depover, R Petrov, K Verbeken (2017) Influence of sample geometry and microstructure on the hydrogen induced cracking characteristics under uniaxial load. Materials Science and Engineering: A 690: 88-95.
35. Laureys, R. Depraetere, M Cauwels, T Depover, S Hertel´e, K Verbeken (2022) Use of existing steel pipeline infrastructure for gaseous hydrogen storage and transport: A review of factors affecting hydrogen induced degradation. Journal of Natural Gas Science and Engineering 101: 104534.
36. M Bruchhausen, S Holmström, JM Lapetite, S Ripplinger (2017) On the determination of the ductile to brittle transition temperature from small punch tests on Grade 91 ferritic-martensitic steel. International Journal of Pressure Vessels and Piping 155: 27-34.
37. (2007) Small punch test method for metallic materials. CEN Workshop Agreement CWA, p. 15627.
38. M Milad, N Zreiba, F Elhalouani, C Baradai (2008) The effect of cold work on structure and properties of AISI 304 stainless steel. Journal of Materials Processing Technology 203(1-3): 80-85.
39. V Shrinivas, SK Varma, LE Murr (1995) Deformation-induced martensitic characteristics in 304 and 316 stainless steels during room-temperature rolling. Metallurgical and Materials Transactions A 26: 661-671.